Development 133, 107-115 doi:10.1242/dev.02182

Heart and soul/PRKCi and nagie oko/Mpp5 regulate myocardial coherence and remodeling during cardiac morphogenesis

Stefan Rohr[1], Nana Bit-Avragim[1,2] and Salim Abdelilah-Seyfried[1,*]

Organ morphogenesis requires cellular shape changes and tissue rearrangements that occur in a precisely timed manner. Here, we show that zebrafish heart and soul (Has)/protein kinase C iota (PRKCi) is required tissue-autonomously within the myocardium for normal heart morphogenesis and that this function depends on its catalytic activity. In addition, we demonstrate that nagie oko (Nok) is the functional homolog of mammalian protein associated with Lin-seven 1 (Pals1)/MAGUK p55 subfamily member 5 (Mpp5), and we dissect its earlier and later functions during myocardial morphogenesis. Has/PRKCi and Nok/Mpp5 are required early for the polarized epithelial organization and coherence of myocardial cells during heart cone formation. Zygotic *nok/mpp5* mutants have later myocardial defects, including an incomplete heart tube elongation corresponding with a failure of myocardial cells to correctly expand in size. Furthermore, we show that *nok/mpp5* acts within myocardial cells during heart tube elongation. Together, these results demonstrate that cardiac morphogenesis depends on the polarized organization and coherence of the myocardium, and that the expansion of myocardial cell size contributes to the transformation of the heart cone into an elongated tube.

KEY WORDS: Organ morphogenesis, *prkci*, Myocardium, *heart and soul*, *nagie oko*, *mpp5*, *pals1*, Zebrafish

INTRODUCTION

Vertebrate heart morphogenesis involves the generation of a simple tube that is shaped into a complex functional organ. The types of cellular and tissue rearrangements driving this process are largely unknown. In zebrafish, heart morphogenesis involves the fusion of two bilateral populations of cardiac progenitor cells at the midline of the embryo followed by the formation of the three-dimensional heart cone, a transitional structure that consists of a dorsal ventricular and a ventral atrial part (Fig. 1A) (Stainier et al., 1993; Yelon et al., 1999). Subsequently, the heart cone moves from the dorsoventral into the anterior-posterior plane, a process referred to as tilting. As a consequence, the ventricular portion of the heart cone comes to lie more posteriorly. Finally, the heart cone elongates along the anterior-posterior axis into the heart tube, which is converted into a looped, two-chambered organ.

The *heart and soul* (*has*) mutation causes severe defects in cardiac morphogenesis, in which tilting of the heart cone is blocked and heart tube elongation is impaired (Yelon et al., 1999; Horne-Badovinac et al., 2001; Peterson et al., 2001). The *has* gene encodes PRKCi, which is required for the establishment of apicobasal polarity of epithelial cells. PRKCs are components of the apical Par3 protein complex, which has been linked to the apical Crumbs-Pals1/Mpp5 protein complex (Hurd et al., 2003; Nam and Choi, 2003; Wang et al., 2004). Consistent with a function in apicobasal cell polarity, *has* mutants show defective formation and maintenance of several embryonic epithelia. This observation led us to investigate whether an epithelial tissue is involved in cardiac morphogenesis. As heart cone tilting and heart tube elongation occur in *cloche*, a zebrafish mutant that lacks endocardial cells, morphogenesis may largely depend on the myocardium or on tissues external to the heart (Stainier et al., 1995). During heart fusion and cone formation, myocardial cells are organized into two bilateral cell populations that have some characteristics of polarized epithelia (Trinh and Stainier, 2004; Trinh et al., 2005). At these early stages, PRKCs are localized to the apical junctions of myocardial cells.

In this study, we expand on the roles of *nagie oko* (*nok*)/*mpp5* and *has*/*prkci* during polarization of the myocardial layer and cardiac morphogenesis. We show that *has*/*prkci* and *nok*/*mpp5* function within myocardial cells during heart cone formation and that Has/PRKCi function requires its catalytic activity. Loss of *has*/*prkci* disrupts the epithelial organization of myocardial cells and blocks heart cone tilting. Using *nok*/*mpp5* antisense morpholino oligonucleotides (MO), we have identified an early function of this gene in epithelial polarity of myocardial cells before heart cone formation, whereby heart cone fusion is severely impaired. Moreover, zygotic *nok*/*mpp5* mutants display defects in myocardial remodeling that contribute to the subsequent elongation of the heart tube.

MATERIALS AND METHODS

Fish maintenance and stocks

Zebrafish were maintained at standard conditions (Westerfield, 1994). Embryos were staged by hours post-fertilization (hpf) at 28.5°C (Kimmel et al., 1995) and according to somite number. The nok^{m520} allele analyzed in this study results in a premature stop codon at residue Arg 546 within the GUK domain (Wei and Malicki, 2002), whereas nok^{s305} causes the loss of the entire GUK domain, resulting in an even larger truncation (Wei, personal communication). The nok^{m520} mutation has been shown to cause a complete, or almost complete, loss of function (Wei and Malicki, 2002). Moreover, the nok^{s305} mutation placed in trans to the nok^{m520} mutation produced a phenotype that was indistinguishable from nok^{s305} homozygotes. Therefore, the nok^{s305} mutation causes a complete, or almost complete, loss of function.

The *Tg*(*cmlc2:prkci*) and *Tg*(*cmlc2:nok*) transgenic lines were generated by injection of I-*Sce*I *cmlc2:prkci* and I-*Sce*I *cmlc2:nok* transformation vectors into 1-cell stage embryos (Thermes et al., 2002). F1 founders were

[1]Max Delbrück Center (MDC) for Molecular Medicine, Robert-Rössle Strasse 10, 13125 Berlin, Germany. [2]The Charité, Department of Cardiology, Campus Buch and Campus Virchow Clinics, Humboldt University, Berlin, Germany.

*Author for correspondence (e-mail: salim@mdc-berlin.de)

Accepted 25 October 2005

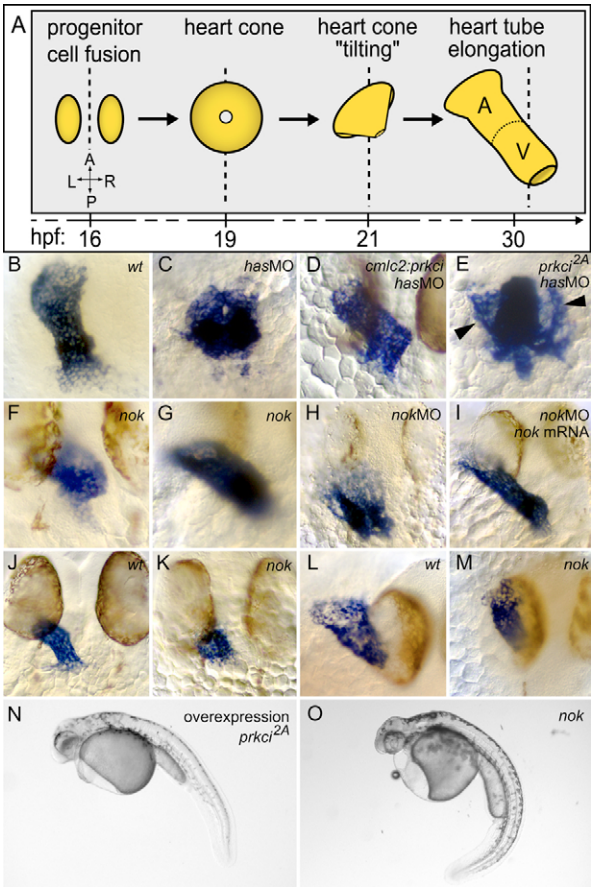

Fig. 1. Cardiac morphogenesis in different genetic backgrounds. (**A**) Depiction of several key stages of zebrafish heart formation, beginning with the juxtaposition of two bilateral cardiac progenitor cell populations along the midline of the embryo (dotted line) to the elongation of the heart tube along the anterior-posterior axis. Dorsal view onto heart field. See text for detailed explanations. (B-I) *cmlc2*, (J,K) *vmhc* and (L,M) *amhc* expression. Embryos are 30-32 hpf. Parts L and M were captured with a 30° angle from dorsal for better visualization of atrial morphology. (**B-D**) Comparison of wild-type, *has/prkci* morphant and *Tg*(*cmlc2:prkci*) transgenic and *has/prkci* morphant embryos. (**E**) Heart cone formation is not completed, resulting in bilateral wings of myocardial progenitor cells (arrowheads) in *prkci*^{2A} kinase-dead mutants. (**F**,**G**) Heart cone 'tilting' occurs, but heart tube elongation is delayed to varying degrees in *nok* mutants. (F) Severe and (G) medium-strength phenotypes. (**H**) *nok/mpp5* morphants display a severe heart tube elongation defect. (**I**) Co-injection of *nok/mpp5* MO with wild-type *nok/mpp5* mRNA rescues myocardial morphogenesis. There is no developmental delay. (**J**,**K**) Length of the ventricle is affected in *nok* mutants. (**L**,**M**) Length of the atrium is shortened and, along the mediolateral axis, narrower than wild type. (**N**,**O**) *nok*^{s305} mutants and embryos that express high levels of PRKCi^{2A} mutant protein (overexpression phenotype) are phenotypically similar. The body axis is curved ventrally and the retinal pigmented epithelium is largely disrupted, leaving the central portion of the retina uncovered, a phenotype more severe than in *has* mutants.

identified by PCR genotyping and used for the establishment of stable lines. For rescue experiments using the transgenic lines in *has* or *nok* mutant backgrounds, respectively, embryos were PCR genotyped for the presence of the transgene insertion using transgene-specific primers (primer sequence information available upon request).

Clonal analysis of mRFP-positive cells was performed by DNA injection using an I-SceI vector containing an *cmlc2:mRFP* insert. The statistical significance of the data was evaluated using Student's *t*-test function on Excel software.

DNA constructs and site-directed mutagenesis

The coding region of zebrafish *has/prkci* was amplified by PCR from a full-length clone (Horne-Badovinac et al., 2001), introducing *Xho*I and *Xba*I restriction sites 5′ and 3′, respectively, and subcloned into the expression vector pCS2+. Site-directed mutagenesis was performed using the Quick Change Site Directed Mutagenesis Kit (Stratagene, CA, USA).

Mutagenesis primer sequences used for *PRKCi*^{2A}

5′-CCCAATTACATTGCAGCAGCGATTCTGAGAGGAGAAG-3′.

Further details are available upon request. pXT7NOK containing full-length *nok* was a gift from J. Malicki (Massachusetts General Hospital, Boston, MA). The *cmlc2:mRFP* was cloned by introducing the PCR-amplified *mRFP* fragment into the I SceI *cmlc2* transformation vector.

RNA and morpholino injections

Constructs were transcribed using the SP6 MessageMachine kit (Ambion). In vitro synthesized capped mRNA was dissolved in water and mixed with the MO prior to injection. Typically, 60 pg of RNA were injected into WIK or WIK/TL embryos. For overexpression, 120 pg of *prkci*^{2A} were injected into wild-type embryos. MOs (Gene Tools) were injected at a concentration of 100 μmol/l. MO sequences were: *nok*MO, 5′-TGAGGTCAGCAGC-GGCTCCAAACAC-3′; *has*MO, 5′-TGTCCC-GCAGCGTGGGCATTATGGA-3′.

In situ hybridization

Whole-mount in situ hybridization was performed as previously described (Jowett and Lettice, 1994). Digoxigenin-UTP-labeled riboprobes were synthesized according to the manufacturer's instructions (Boehringer Mannheim). The *cmlc2* probe (AF114428) was amplified from cDNA and subcloned into pCS2+. Probes for *amhc* and *vmhc* were a gift from D. Yelon. Embryos were mounted in Permount (Fisher Scientific) and documented using an Axioplan 2 microscope (Zeiss). Images were processed with Adobe Photoshop software (Adobe Systems).

Antibody and phalloidin staining

Antibody and phalloidin stainings were performed as previously described (Horne-Badovinac et al., 2001). Nuclear stainings were performed using SYTOX green nucleic acid stain (Molecular Probes) as described (Picker et al., 1999). The following antibodies were used: rabbit anti-aPKCζ (1:100, Santa Cruz Biotechnology, USA), mouse anti-ZO-1 (1:200, Zymed), rabbit anti-α-catenin (1:200, Sigma), goat anti-rabbit RRX (1:200), anti-mouse Cy5 (1:100) (Jackson ImmunoResearch). Transverse sectioning was performed according to Trinh et al. (Trinh et al., 2004). Hearts were analyzed using a Leica TCS SP2 confocal microscope. For reconstruction of myocardial cell morphology single sections of recorded z-stacks were analyzed using Leica software. For quantification of myocardial cell size, individual scans of *cmlc2:mRFP*-positive cells were analyzed with TINA version 2.08e (Raytest Isotopenmeßgeräte GmbH) and absolute values recalculated as relative values. Standard deviation was calculated using Excel software (Microsoft).

BrdU labeling

Sixteen-somite stage embryos (*nok*^{s305} and wild-type siblings) were yolk injected with 10 mmol/l BrdU in 0.2 mol/l KCl. Embryos were fixed at 32 hpf in 4% PFA for 2 hours at RT. After rinsing in 1× PBS, embryos were dehydrated in MeOH and stored overnight at –20°C. After rehydration, the samples were digested in 10 μg/ml proteinase K for 15 minutes and refixed

in 4% PFA for 20 minutes. Incubation in 2N HCl for 1 hour was performed to relax the chromatin and facilitate the following immunolabeling using anti-BrdU antibody (Roche 1170376) diluted 1:100 in blocking solution. BrdU was visualized with Cy3-conjugated goat anti-mouse (Jackson ImmunoResearch; 1:500).

Apoptosis detection by TUNEL staining

The fragmented DNA of apoptotic cells was detected in 32-hpf-old *nok*^{s305} and wild-type siblings using the In Situ Cell Death Detection Kit TMR Red (Roche) following the protocol from Shepard et al. (Shepard et al., 2004), with the exception that the yolk was removed manually after fixation for improved accessibility to the heart.

Microangiography

Microangiographic images were generated by injection of 70 kD FD into the dorsal aorta of 36-hpf embryos. Embryos were imaged 5-10 minutes after injection with a CoolSnap ES camera (Photometrics). Data were collected and analyzed using Metamorph software version 6.1 (Visitron Systems).

RESULTS

Has/PRKCi functions tissue-autonomously within the myocardium during heart morphogenesis

To test our hypothesis that Has/PRKCi regulates cardiac morphogenesis intrinsically within the myocardium, we generated a line of transgenic zebrafish that expresses wild-type PRKCi under the control of the *cardiac myosin light chain 2* (*cmlc2*) promoter region within all myocardial cells [*Tg*(*cmlc2:prkci*)]. Translation of the transgene expression is insensitive to the *has*/*prkci* MO used in this study. We used *cmlc2*, a marker for cardiac differentiation (Yelon et al., 1999), to assess heart morphogenesis. Within *Tg*(*cmlc2:prkci*) transgenic embryos, injection of the *has*/*prkci* MO produced the complete range of epithelial defects characteristic of *has*/*prkci* but failed to affect cardiac morphogenesis (Fig. 1D). *has*/*prkci* morphants that were *Tg*(*cmlc2:prkci*) transgenic showed correct heart cone tilting followed by heart tube elongation. In total, we examined cardiac morphogenesis in 61 transgenic embryos, 41 of which produced an elongated heart tube (65.1%). By contrast, almost all of the control wild-type siblings injected with *has*/*prkci* MO produced the *has*/*prkci* cardiac morphogenesis phenotype with an arrested heart cone (Fig. 1C). The variability of heart morphogenesis rescue among *Tg*(*cmlc2:prkci*) embryos may be due to the critical period of *has*/*prkci* function, which coincides with the onset of *cmlc2* transgene expression. Previously, the promoter region used for the production of the transgenic line has been shown to display a variable onset of transgene expression (Huang et al., 2003). Therefore, Has/PRKCi acts tissue-autonomously within myocardial cells and is sufficient for correct heart cone tilting and heart tube elongation.

To test whether Has/PRKCi activity within myocardial cells is sufficient for heart function in an otherwise morphant embryo, we injected 70 kD fluorescein dextran into the dorsal aorta of 36-hpf embryos and found that peripheral circulation was indeed present, which is never seen in *has*/*prkci* morphants (Fig. 2B,C). A similar result was obtained after outcross of the transgene into the *has* mutant background (Fig. 2E,F). Therefore, Has/PRKCi activity within myocardial cells is sufficient for heart function.

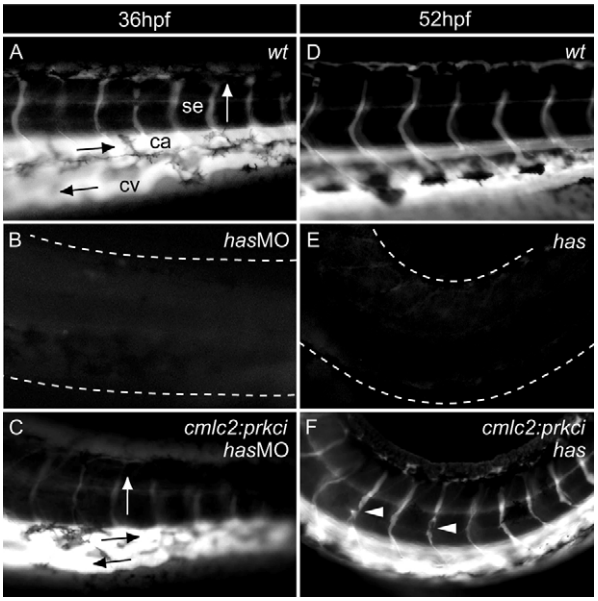

Fig. 2. Has/PRKCi activity within myocardial cells is sufficient for heart function. Microangiograms depicting the peripheral circulation present within the tail region of embryos. The direction of blood flow is indicated by arrows. (**A**) wild-type embryo at 36 hpf. (**B**) *has/prkci* morphant at 36 hpf. (**C**) *Tg*(*cmlc2:prkci*) transgenic animal injected with the *has/prkci* MO at 36 hpf. (B) By contrast, peripheral circulation is never seen in *has/prkci* morphants. (**D**) Wild-type embryo at 52 hpf, with robust circulation. (**E**) Complete lack of peripheral circulation in a *has* mutant. (**F**) At 52 hpf, peripheral circulation is present in *has* mutants with *Tg*(*cmlc2:prkci*) insertion but defects in vessel formation can be observed (arrowheads). The white dotted line indicates the outline of the tail region. ca, caudal aorta; cv, caudal vein; se, segmental vessel.

Heart morphogenesis requires the catalytic activity of Has/PRKCi

To further assess whether Has/PRKCi function during heart morphogenesis depends on its kinase activity, we generated a mutation of *has*/*prkci* that encodes a kinase-dead version of the protein (*prkci*^{2A}; residues Pro 408 and Glu 409 within the catalytic center exchanged for Ala) (Hanks and Hunter, 1995). Whereas co-injection of 60 pg of wild-type *prkci* mRNA together with *has*/*prkci* MO gave a complete rescue (data not shown), co-injection of *prkci*^{2A} mRNA with *has*/*prkci* MO resulted in the *has*/*prkci* external phenotype. We refer to these animals as *prkci*^{2A} mutants. The 32-hpf wild-type heart is an elongated two-chambered tube with posterior ventricle and anterior atrium, one-third of *prkci*^{2A} mutants had the characteristic dysmorphic cone-like heart of *has*/*prkci* mutants. Thus, normal morphogenetic movements of heart cone tilting and regular elongation into the two-chambered heart tube had failed. Moreover, 54% of *prkci*^{2A} mutants displayed an even more severe phenotype in which cardiac fusion was not completed, resulting in bilateral wings of cells (Fig. 1E). Therefore, the *prkci*^{2A} mutation affects earlier steps of heart morphogenesis than the zygotic *has*/*prkci* mutation, which we attribute either to an interference with maternal Has/PRKCi protein or redundant function of PRKCζ. Thus, the biological activity of Has/PRKCi during heart morphogenesis crucially depends on its catalytic kinase activity within myocardial cells.

Nok is the functional homolog of mammalian Pals1/Mpp5 and is required for heart morphogenesis

To test whether *has*/*prkci* cardiac morphogenesis defects are attributed to defective epithelial cell polarity, we investigated whether other regulators of epithelial cell polarity cause similar defects. As overexpression of *prkci*^{2A} mRNA in wild-type

embryos produced a phenotype similar to that of *nok* mutants (Fig. 1N,O), we first characterized the role of this gene in cardiac morphogenesis. The *nok* gene encodes a membrane-associated guanylate kinase (MAGUK) with 68% identity to mammalian Pals1/Mpp5 and is required for the maintenance of epithelial cell polarity (Wei and Malicki, 2002; Horne-Badovinac et al., 2003). In mammalian cells, Pals1/Mpp5 functions as a scaffolding protein that links the transmembrane receptor Crumbs with Par6-PRKC (Hurd et al., 2003; Wang et al., 2004). We tested whether Nok is a functional homolog of mammalian Pals1/Mpp5 by injecting murine *Pals1/MPP5* mRNA into *nok* mutants and morphants. Murine *Pals1/MPP5* mRNA largely prevented ventral curvature of morphants (n=29/30 morphants rescued; Fig. 3A-C). To further evaluate the rescue efficiency of *Pals1/MPP5* mRNA, we assayed the organization of the retinal pigmented epithelium (RPE), which is almost completely lost in *nok* mutants but was significantly recovered upon injection of murine *Pals1/MPP5* mRNA (Fig. 3D-F). Finally, we assessed the recovery of heart function by quantifying the presence of circulation within peripheral blood vessels in *nok* morphants at 36 hpf. Injection of *Pals1/MPP5* mRNA caused a significant increase in the number of *nok/mpp5* morphants with functional circulation (Fig. 3G). The failure to completely rescue the *nok* morphant phenotype may be attributed to sequence variations between Nok and murine Pals1. Therefore, Nok is a functional homolog of murine Pals1/Mpp5.

Assessment of heart morphology in *nok/mpp5* mutant hearts (*nok*^{s305} and *nok*^{m520} alleles) revealed that they largely developed beyond the cone stage. However, expression of *cmlc2* showed that the heart failed to completely elongate by 36 hpf. The defects observed ranged from severe (the heart tube failed to elongate) (Fig. 1F) to moderate (the heart tube was significantly shorter than wild type) (Fig. 1G) to mild (the heart tube elongated but was narrow) (not shown). Expression of *ventricular myosin heavy chain* (*vmhc*) and *atrial myosin heavy chain* (*amhc*) revealed that chamber-specific differentiation occurred but that both the atrium and the ventricle were defective in size and form (Fig. 1J-M) (Berdougo et al., 2003). Therefore, we conclude that *nok/mpp5* is required for correct heart tube elongation.

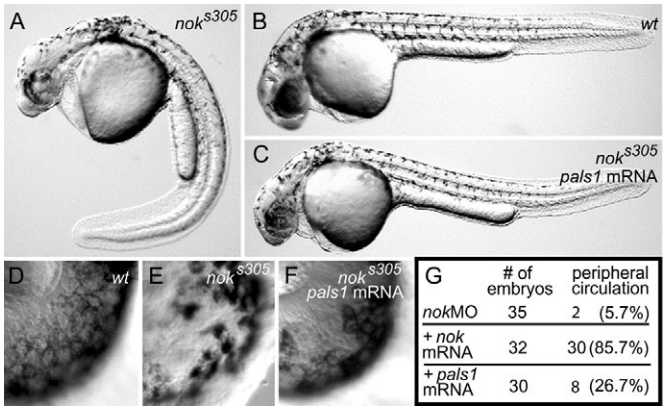

G	# of embryos	peripheral circulation
*nok*MO	35	2 (5.7%)
+ *nok* mRNA	32	30 (85.7%)
+ *pals1* mRNA	30	8 (26.7%)

Fig. 3. Nok is the functional homolog of mammalian Pals1/Mpp5. (**A**) *nok*^{s305} mutant with ventrally curved body form and severely disrupted retinal pigmented epithelium at 34-36 hpf. (**B**) Wild type. (**C**) Murine *Pals1/Mpp5* mRNA results in a partial phenotypic rescue of *nok*^{s305} mutants, including the body form. (**D**) Wild-type retinal pigmented epithelium. (**E**) The *nok*^{s305} retinal pigmented epithelium is severely disrupted. (**F**) Retinal pigmented epithelial cells are coherent in *Pals1* mRNA-injected *nok*^{s305} mutants (partial rescue). (**G**) A summary table showing the percentages of embryos with peripheral circulation among *nok* morphants injected with 50 ng/μl wild-type *nok* or 50 ng/μl *Pals1/Mpp5* mRNA.

has/prkci and *nok/mpp5* are required for coherence and polarized organization of the myocardium during heart cone formation

We tested whether *nok/mpp5* has a function prior to heart tube elongation by injecting a 5′-UTR-directed MO that has previously been shown to completely eliminate maternal and zygotic protein expression by the second day of development (Wei and Malicki, 2002). Similarly, for *has/prkci*, we injected an ATG-directed MO that has been shown to eliminate protein expression (Horne-Badovinac et al., 2001). Indeed, myocardial morphogenesis in these morphants resembled the *has/prkci* mutant heart phenotype (see below). The co-injection of *nok/mpp5* MO with wild-type *nok/mpp5* mRNA completely rescued myocardial morphogenesis, thereby demonstrating that the MO causes a specific developmental defect (Fig. 1I).

To assess the effects of *nok/mpp5* and *has/prkci* on the polarization of the myocardial epithelium, we used a transgenic line of zebrafish that expresses green fluorescent protein (GFP) under the control of the *cmlc2* promoter region [*Tg*(*cmlc2:GFP*)] to visualize heart morphology (Huang et al., 2003). We utilized this transgenic line in conjunction with antibodies against the junctional protein Zonula occludens-1 (ZO-1), against PRKCi and z (anti-aPKC) at the apical junction of myocardial cells and α-catenin at the adherens junction and lateral membranes, and rhodamine phalloidin to detect filamentous actin. In wild type, before heart cone formation (16-somite stage), myocardial cells were positioned in two bilateral sheets that converged toward the midline (Fig. 4A). Within each bilateral sheet, myocardial cells were highly polarized and displayed junctional belts positive for PRKC and ZO-1 (Fig. 4J,K) (Trinh and Stainier, 2004; Trinh et al., 2005). Within the next 2 hours, myocardial cells converged onto the midline and fused to form the heart cone (20-somite stage; Fig. 4B). At this stage, the myocardium was a monolayered epithelial sheet that lay symmetrically near the midline and had the appearance of an evenly shaped cone structure with PRKC- and ZO-1-positive junctional belts. In transverse sections, lateral portions of the myocardium were organized as a monolayered sheet of mostly cuboidal cells. There was asymmetrical localization of ZO-1 at the apical side and PRKC just basal of ZO-1 and more diffusely along basolateral membranes (Fig. 5B). The adherens junctional protein, α-catenin, largely co-localized with ZO-1 at the apical membrane (Fig. 5D).

Before heart cone tilting, myocardial cells further converged and the heart cone elongated along the dorsoventral axis (Fig. 4C). During tilting (Fig. 4D), the wild-type heart cone became highly asymmetrical and revealed the presence of several morphologically elongated myocardial cells that were attached to surrounding tissues (Fig. 4S). These cells were located at the anterior/ventral edge of the heart cone.

In *has/prkci* and *nok/mpp5* morphants, the epithelial organization of the myocardium was affected already before heart cone formation (16-somite stage). The localization of ZO-1 was in a spotted distribution rather than in a contiguous junctional belt (Fig. 4N,P). Moreover, within *nok/mpp5* morphant myocardial cells, PRKC was mislocalized in a diffuse pattern (Fig. 4M). Transverse sections revealed that *nok/mpp5* and *has/prkci* morphant myocardial layers appeared less coherent and were, in part, multilayered (Fig. 5C,E). Both morphants

lacked the asymmetric apical distribution of ZO-1, which was, instead, found to be diffusely distributed. Moreover, PRKC was mislocalized in a diffuse pattern in *nok/mpp5* morphants (Fig. 5C). In *has/prkci* morphants, there was no co-localization of ZO-1 and α-catenin. Instead, α-catenin was diffusely distributed along the membrane (Fig. 5E). Therefore, Nok/Mpp5 functions to maintain PRKC localization basal of ZO-1. The coherence of the myocardial sheets was disrupted and heart cone fusion was delayed in *nok/mpp5* morphants (Fig. 4E,G). Indeed, *nok/mpp5* morphants failed to undergo heart cone fusion at the 28-somite stage (Fig. 4G), a stage at which the wild-type heart cone has already tilted into the anterior-posterior plane of the embryo (Fig. 4D). In *has/prkci* morphants, the coherence of the myocardial layer was affected as indicated by holes that disrupt the integrity of this layer (Fig. 4H). Moreover, tilting of the heart cone did not occur. Myocardial cells that connect the myocardium with surrounding tissues were not seen in *has/prkci* mutants. We conclude that the polarized epithelial organization and coherence of the myocardium is affected in *has/prkci* and *nok/mpp5* morphants. Therefore, *nok/mpp5* morphants reveal an early gene function that is not apparent in the two zygotic mutants characterized.

Zygotic *nok/mpp5* is required for correct myocardial cell number and myocardial remodeling during heart tube elongation

To further investigate the zygotic role of *nok/mpp5* in myocardial morphogenesis, we characterized the heart tube elongation defects. Defective heart tube elongation in *nok/mpp5* mutants may result because of an altered cellular architecture of the myocardial layer, fewer cells, or a combination of the two. To distinguish among these possibilities, we first counted myocardial cells at 36 hpf in confocal sections of wild-type and nok^{s305} mutant embryos that were also *Tg(cmlc2:GFP)* transgenic. Individual myocardial cells are identifiable by the presence of a strong nuclear GFP expression (Fig. 6A,B). Wild-type hearts had, on average, 28% more myocardial cells than nok^{s305} mutant hearts [wild type, 269±13 s.d. (n=3 hearts); nok^{s305}, 211±19 s.d. (n=6 hearts)]. This difference could account for part of the heart tube elongation defects in *nok/mpp5*.

A smaller cell count may be caused by a reduced rate of cell proliferation or by an increased rate of cell death. We first compared the proliferation rates of wild type and *nok/mpp5* mutants that were also *Tg(cmlc2:GFP)* transgenic using a BrdU assay. The mitotic index of myocardial cells (mitotic cells/100 myocardial cells) that divided between the 16-somite stage and 32 hpf was similar

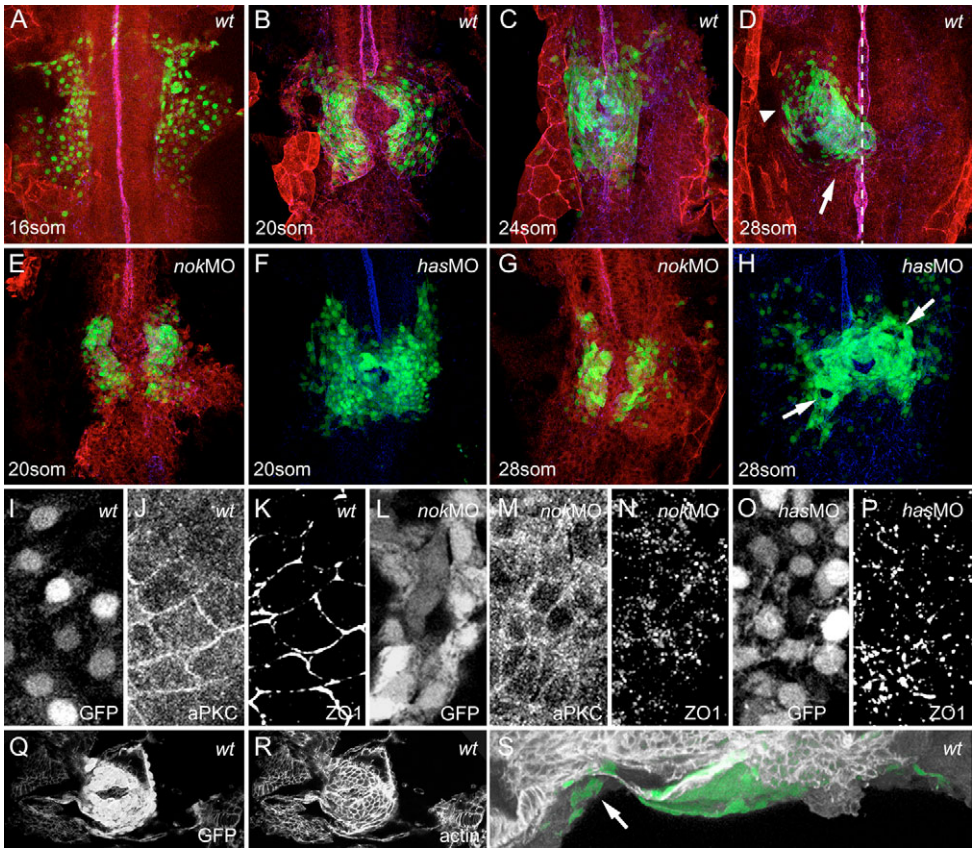

Fig. 4. Myocardial epithelial organization is disrupted in *has/prkci* and *nok/mpp5* morphants. All images represent reconstructions of confocal Z-stack sections imaged on whole mounts. (A-E,G) cmlc2:GFP, green (nuclear GFP within myocardial cells); PRKC/aPKC, red; ZO-1, blue. PRKC and ZO-1 were used as a counterstain to visualize the embryonic midline (see also dotted line in D). (F,H) cmlc2:GFP, green and ZO-1, blue. (Q-S) cmlc2:GFP and filamentous actin. (**A**) At the 16-somite stage, wild-type myocardial cells are organized into two bilateral sheets of cells. (**B**) Both sheets converge onto the midline, where they fuse to form the heart cone around the 20-somite stage. (**C**) Further convergence leads to a narrowing of the heart cone and expansion along the dorsoventral axis around the 24-somite stage. The entire heart cone moves out of the midline toward the left and anterior. (**D**) Heart cone tilting places the heart into the anterior-posterior orientation by the 28-somite stage. The atrium (arrowhead) is located to the left and anterior whereas the ventricle (arrow) is oriented toward the midline and posterior. (**E**,**G**) *nok/mpp5* morphants display a delay in myocardial fusion to form the heart cone. (**F**,**H**) *has/prkci* morphants undergo heart cone fusion at the midline but tilting of the heart cone into the anterior-posterior orientation fails. Note the disrupted appearance of the myocardial layer, with holes and rough edges (arrows). (**I-P**) All images are details of confocal reconstructions of confocal Z-stacks imaged from 16-somite stage whole mounts, separated into the individual channels. (I-K) At the 16-somite stage, wild-type myocardial cells have an epithelial organization with junctional distribution of PRKC and ZO-1. (L-N) At the 16-somite stage, *nok/mpp5* morphants display a diffuse distribution of PRKC along membranes and ZO-1 junctional belts are disrupted and appear as spots. (O,P) At the 16-somite stage, *has/prkci* morphants display a spotted distribution of ZO-1. (**Q**,**R**) Dorsal view onto the heart cone shown in S. (**S**) During tilting, specialized elongated myocardial cells containing actin-cables attach the heart cone to surrounding tissues (see arrow). Orientation: dorsal view and anterior to the top, except in S, lateral view and anterior to the left.

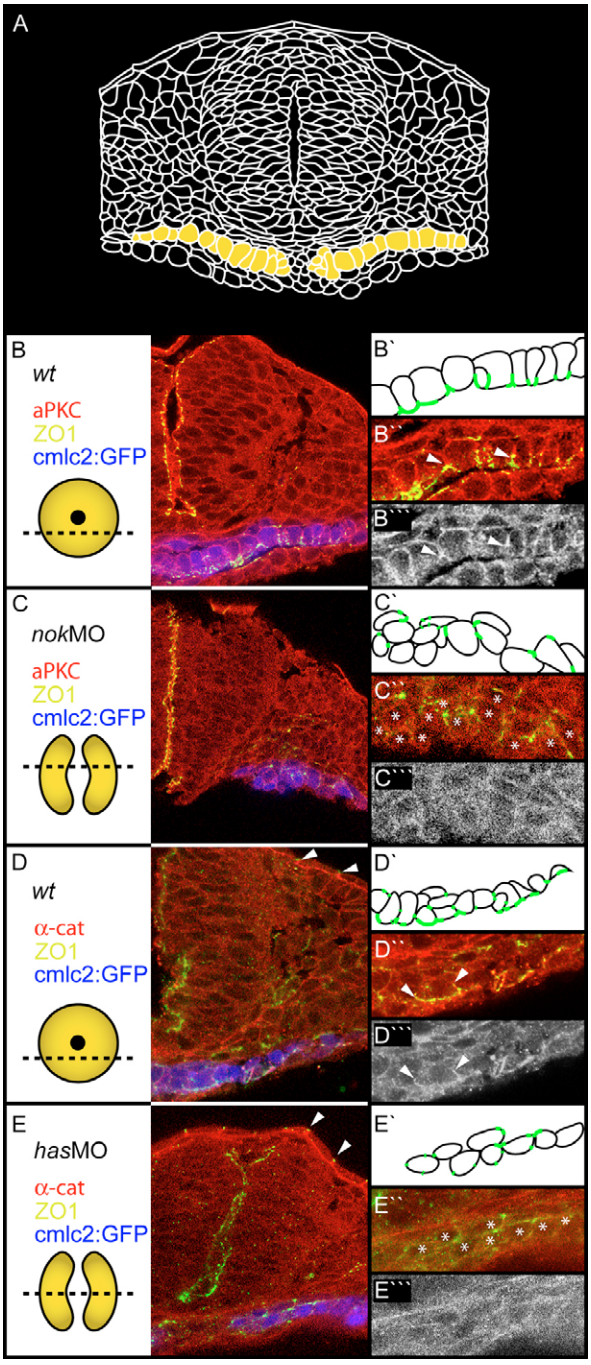

Fig. 5. Apicobasal polarity is disrupted in *has*/*prkci* and *nok*/*mpp5* morphants. Transverse sections of heart cone stage (20-somites) embryos. The section plane is indicated in each case (dotted lines). PRKC/aPKC and α-catenin, red or gray; ZO-1, green; GFP false colored in blue. (**A**) Drawing of a transverse section through the center of the heart cone. Two bilateral wings of myocardial cells are indicated in yellow. (**B**,**B′′**) In wild type, ZO-1 is localized to the apical membranes of the monolayered myocardial cell layer. (**B′′′**) PRKC is localized basal of ZO-1 (see arrowheads). (**C**,**C′′**) *nok* morphants display diffusely positioned spots of ZO-1. (**C′′′**) PRKC is mislocalized in a diffuse pattern. (**D**,**D′′**,**D′′′**) Co-localization of ZO-1 and α-catenin at the apical membrane in wild type. (**E**,**E′′**,**E′′′**) In *has* morphants, co-localization of ZO-1 and β-catenin is lost. The peridermal localization of ZO-1 and α-catenin is not affected (arrowheads). (E′′′) α-catenin is diffusely distributed along the membrane. Stars indicate myocardial cells.

between wild type (10.9%) and *nok*/*mpp5* mutants (10.3%) [wild type, 29.3±8.3 s.d. BrdU-positive cells/heart (*n*=10 hearts); *nok*/*mpp5*, 21.8±15.1 s.d. BrdU-positive cells/heart (*n*=6 hearts)] (Fig. 6H,I,L). Therefore, cell proliferation contributes only slightly to heart tube elongation between the 16-somite stage and 32 hpf, and the comparable mitotic index does not explain the differences in cell numbers of wild-type and *nok*/*mpp5* mutant myocardia. We next tested whether an increased rate of cell death might cause the reduced myocardial cell count in *nok*/*mpp5* mutants. TUNEL analysis of wild type and *nok*/*mpp5* mutants that were also *Tg*(*cmlc2:GFP*) transgenic indicated a low rate of apoptotic cell death that was slightly increased in mutants [wild type, 0.5±1.0 s.d. TUNEL-positive cells/heart (*n*=10 hearts); *nok*/*mpp5*, 2.0±1.2 s.d. TUNEL-positive cells/heart (*n*=10 hearts)] (Fig. 6J,K,L). Similar results were obtained with Acridine Orange stainings (not shown). Therefore, the smaller cell count in *nok*/*mpp5* mutants is not caused by a reduced cell proliferation rate or increased rates of apoptotic cell death during heart tube elongation. We suggest that a smaller heart is the result of altered proliferation and/or cell survival rates at earlier stages of cardiogenesis, or a smaller pool of progenitor cells.

Next, we analyzed the epithelial organization of myocardial cells at 36 hpf. At this stage, myocardial cells within the atrial/anterior portion of the heart tube had extended cell sizes and nuclei were distantly spaced, whereas myocardial cells within the posterior/ventricular portion of the heart tube were more narrowly spaced (Fig. 6A). Whereas atrial myocardial cells acquired elongated squamous epithelial shapes (Fig. 6A′′,C), ventricular myocardial cells had a cuboidal epithelial organization (Fig. 6A′).

Next, we compared the spatial arrangement of myocardial cells and found that *nok*/*mpp5* mutant myocardial cells were more densely arranged than wild-type cells at 36 hpf. The differences were most striking within the atrium, where *nok*/*mpp5* mutant myocardial cells were reminiscent of wild-type heart-cone-stage myocardial cells.

For visualization and measurement of individual myocardial cell shapes in wild type and *nok*/*mpp5* mutants, we used an expression plasmid [*cmlc2:membrane red fluorescent protein* (*cmlc2:mRFP*)] to achieve transient and mosaic expression of mRFP within single myocardial cells. We compared single cells expressing mRFP between wild-type siblings and mutants within the *Tg*(*cmlc2:GFP*)/*nok*^{s305} and *Tg*(*cmlc2:GFP*)/*nok*^{m520} transgenic backgrounds (Fig. 6E-G). The relative surface extension of mRFP-positive cells was quantified using TINA 2.08 software (Raytest Isotpenmeßgeräte GmbH). In summary, we found that wild-type myocardial cells were on average about 25-35% more extended than in *nok*/*mpp5* [wild type, 100±25.4% s.d. (*n*=53 cells); *nok*^{s305}, 74.1±25.3% s.d. (*n*=58 cells); *nok*^{m520}, 64.1±22.6% s.d. (*n*=42 cells)]. The differences in cell surface extension are highly significant ($P \leqslant 0.01$, according to Student's *t*-test). Even more strikingly, wild-type atrial cells had an average surface extension that was about 40% larger than wild-type ventricle cells [wild-type atrium, 136.01±19.48% s.d. (*n*=8 cells); wild-type ventricle, 93.61±20.68% s.d. (*n*=45 cells)]. This demonstrates that the average wild-type ventricular cell is more extended than the average *nok*/*mpp5* mutant myocardial cell (the average surface extension of mutant cells being derived from both atrial and ventricular myocardial cells). Due to similar cell surface extensions, we did not distinguish between atrial and ventricular cells in *nok*/*mpp5* mutants. In summary, *nok*/*mpp5* mutant myocardial cells do not fully expand in size. Both size reduction of myocardial cells and smaller cell number appear to be

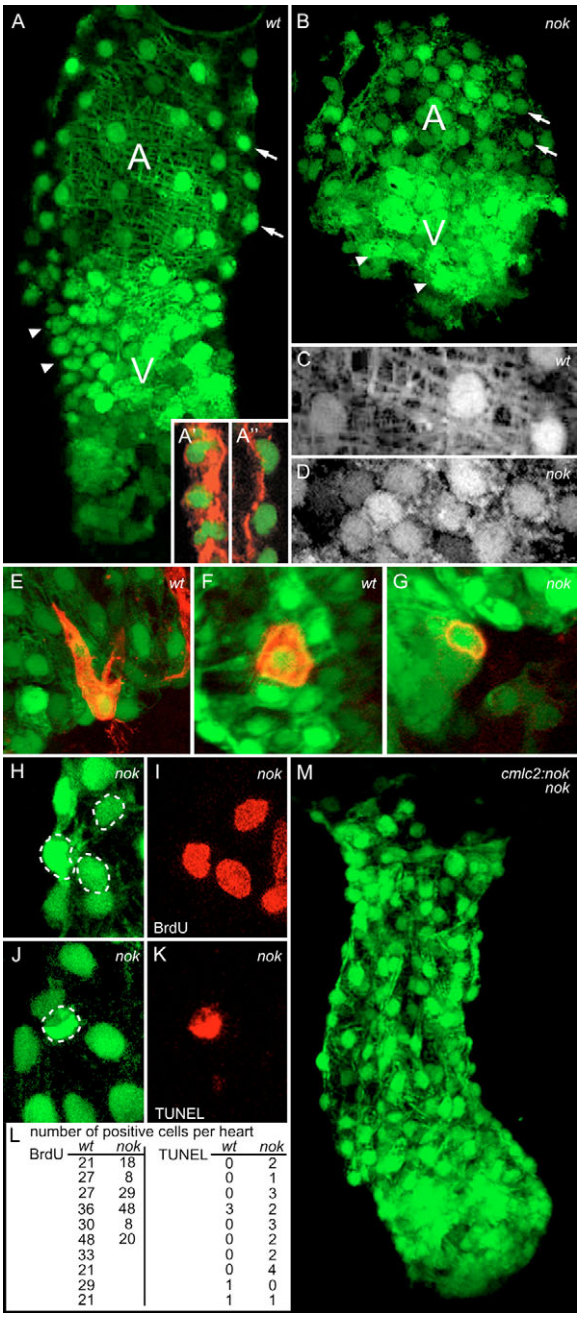

Fig. 6. The zygotic function of *nok/mpp5* is required for myocardial cell remodeling. (A,C,E,F) 36 hpf wild type and (B,D,G) *nok*^{s305} in the *Tg*(*cmlc2:GFP*) transgenic background. (H-K) *nok*^{s305} in the *Tg*(*cmlc2:GFP*) transgenic background at 32 hpf. Images are reconstructions of confocal Z-stack sections. (**A**,**B**) Arrows indicate atrial myocardial cells and arrowheads ventricular myocardial cells. Shape and density of *nok*^{s305} mutant atrial and ventricular cells are similar. (**A′**,**A′′**) Merged confocal serial sections of actin (red) and nuclear stain (SYTOX green nuclear acid stain). (A′) Single sections and fusions of up to three sections of confocal serial stacks show that wild-type ventricular myocardial cells have cuboidal cell shapes. (A′′) wild-type atrial myocardial cells have squamous cell shapes. (**C**,**D**) Comparison of atrial myocardial cells in wild-type and *nok*^{s305} mutant hearts, indicating that *nok*^{s305} mutant atrial myocardial cells fail to expand in size and resemble ventricular myocardial cells. (**E-G**) Mosaic expression of mRFP within single *Tg*(*cmlc2:GFP*) transgenic myocardial cells. (E) Wild-type atrial myocardial cell. (F) Wild-type ventricular myocardial cell. (G) *nok*^{s305} mutant myocardial cell. (**H**,**I**) BrdU analysis of *nok*^{s305} mutant myocardial cells. White dotted lines indicate BrdU-positive cells. (**J**,**K**) TUNEL analysis of *nok*^{s305} mutant myocardial cells. The white dotted line indicates a TUNEL-positive cell. (**L**) Quantification of BrdU- and TUNEL-positive cells. (**M**) *nok/mpp5* functions tissue-autonomously within the myocardium during heart tube elongation. A *nok*^{s305} mutant in the *Tg*(*cmlc2:GFP*) transgenic background that also carries the *Tg*(*cmlc2:nok*) rescue transgene displays an elongated heart tube similar to wild type. Orientation: dorsal view and anterior to the top. A, atrium; V, ventricle.

important factors contributing to heart tube elongation defects in *nok/mpp5* mutants. We conclude that *nok/mpp5* is required for the remodeling of myocardial cells during heart tube elongation.

Nok/Mpp5 functions tissue-autonomously within the myocardium during heart morphogenesis

To test whether *nok/mpp5* is required tissue-autonomously within the myocardium for correct heart tube elongation, we generated a stable transgenic line of zebrafish that expresses wild-type Nok/Mpp5 under the control of the *cmlc2* promoter region *Tg*(*cmlc2:nok*). This transgenic line was introduced into the *nok*^{s305} mutant background that also contained the *Tg*(*cmlc2:GFP*) insertion. Embryos that were homozygous mutant for *nok*^{s305} and displayed the full range of the nok/*mpp5* mutant phenotypes were genotyped by PCR for the presence of the *Tg*(*cmlc2:nok*) insertion. Among 23 transgenic embryos, 15 produced an elongated and rescued heart tube (65.2%). Moreover, whereas in *nok/mpp5* mutants, the inflow tract was mostly obstructed, this phenotype was also rescued in these transgenic animals. This rescue rate is comparable to the rescue efficiency with the *Tg*(*cmlc2:prkci*) transgene and may be attributed to the variable onset of transgene expression under the control of the *cmlc2* promoter region (Huang et al., 2003) (Fig. 6M). Among the homozygous *nok*^{s305} mutants that lacked the rescue transgene, most embryos displayed a shortened and malformed heart tube characteristic of the *nok/mpp5* mutant phenotype (Fig. 6B). Therefore, similar to Has/PRKCi, Nok/Mpp5 functions tissue-autonomously within the myocardial layer.

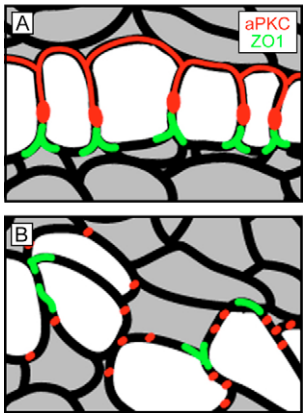

Fig. 7. Correct apicobasal polarity of myocardial cells requires *nok/mpp5*. (**A**) At heart cone stages, myocardial cells are polarized and mostly cuboidal epithelial cells. The junctional marker ZO-1 localizes to the apical side and PRKC (aPKC) just basal of ZO-1 and more diffusely along basolateral membranes. (**B**) The monolayered epithelial organization of myocardial cells and the correct localization of apicobasal polarity markers is disrupted in *nok/mpp5* morphants. However, convergence movements of myocardial cells toward the midline are not affected, suggesting that either epithelial cohesion is not necessary for this type of cell migration or that some epithelial cohesion is maintained.

DISCUSSION

Our data present the first evidence of the role of the apical Crumbs-Nok/Mpp5 complex in heart morphogenesis. We show that zebrafish Nok, which has previously been shown to be required for correct lamination of the neural retina and for the correct polarization of some lateral plate mesodermal cells is a functional homolog of mammalian Pals1/Mpp5 and that it is a regulator of vertebrate embryonic heart morphogenesis (Wei and Malicki, 2002; Horne-Badovinac et al., 2003). Within myocardial cells, Nok/Mpp5 is required for correct junctional localization of Has/PRKCi. We also show that Nok/Mpp5 and Has/PRKCi function autonomously within myocardial cells during heart morphogenesis and that Has/PRKCi function depends on the catalytic kinase activity. Hence, embryonic heart morphogenesis depends on localized Has/PRKCi catalytic activity at the apical junction, and Nok/Mpp5 is essential for its stabilization.

We have demonstrated that *has/prkci* and *nok/mpp5* regulate heart cone tilting, and that *nok/mpp5* also controls the subsequent step of heart tube elongation. The mechanism of heart cone tilting is currently not understood but it is conceivable that a directed motion that displaces the heart cone from the midline toward the left anterior side of the embryo may be involved (compare Fig. 4B,C). This myocardial motion could be caused by an intrinsic motive force and/or by external forces. We have shown that during the process of heart cone tilting myocardial cells are strongly converging to produce a narrow and extended cone that subsequently tilts into the anterior-posterior axis (Fig. 4C). This supports the possibility that myocardial cells are actively moving to cause heart cone tilting and that this movement requires the monolayered, polarized and cuboidal organization of myocardial cells at this stage (Fig. 7). Interestingly, loss of *has/prkci* or *nok/mpp5* does not impede the convergence of myocardial cells toward the midline. Therefore, either heart progenitor cells do not require the integration into an epithelial sheet for migration, or the defective myocardium maintains some epithelial cohesion that is mediated by factors other than the ones tested in our study. We also hypothesize that the morphologically specialized population of myocardial cells that connects the heart cone with surrounding tissues may be necessary to convert external motive forces onto the heart cone or to generate an anchor point that may force the heart cone to always tilt in a stereotypical direction (Fig. 4S).

We have observed that *prkci*^{2A} mutants frequently displayed a myocardial phenotype that was more severe than in *has/prkci* morphants. In fact, overexpression of high levels of *prkci*^{2A} mRNA in wild-type embryos resulted in a phenotype similar to *nok/mpp5* (Fig. 1N,O). Conceivably, PRKCi^{2A} interferes, in a dominant-negative fashion, with pools of maternal Has/PRKCi or another PRKC isoform that is within protein complexes associated with Nok/Mpp5. Immunohistochemistry performed on *has/prkci* mutants using an antibody against the 20 C-terminal amino acids of murine PRKCz demonstrated the presence of another PRKC isoform different from zygotic PRKCi (Horne-Badovinac et al., 2001).

As mammalian Pals1 physically interacts via an evolutionarily conserved region with Par6, and as physical association of the two apical protein complexes, Crumbs-Stardust/Mpp5 and Bazooka-DaPKC-DmPar6, has also been mapped in *Drosophila*, we propose that a similar protein complex is likewise present in zebrafish and that it plays an essential role in zebrafish epithelial maintenance (Wang et al., 2004; Nam and Choi, 2003). The results presented in this study indicate a previously unknown function for these proteins in myocardial polarization and remodeling. The mechanisms by which heart tube elongation is regulated and the contribution of *nok/mpp5* to the remodeling of atrial myocardial cells from a cuboidal shape (at heart cone stages; Fig. 7) to a squamous and elongated shape during heart tube elongation stages currently remain elusive. Moreover, it is possible that cellular rearrangements of myocardial cells during heart tube elongation that are reminiscent of convergence/extension type movements are essential for this process and that they could be regulated by *nok/mpp5*. Further studies into the roles of the apical Crumbs-Nok/Mpp5 and Par6-PRKC protein complexes in this process are warranted.

We thank the members of the Abdelilah-Seyfried laboratory for helpful discussions. Various constructs, antibodies and cDNAs were donations from Walter Birchmeier, Debbie Yelon, Didier Stainier, Klaus Rohr, Jochen Wittbrodt and Reinhard Koestner. Many thanks in particular to Herwig Baier and to members of his laboratory for helping to isolate an additional allele of *nok*, and to Xiangyun Wei for sharing unpublished results. We also thank Ulrike Ziebold, Thomas Willnow and Walter Birchmeier for critical reading of the manuscript. This work was supported in part by a presidential grant from the Helmholtz Society.

References

Berdougo, E., Coleman, H., Lee, D. H., Stainier, D. Y. R. and Yelon, D. (2003). Mutation of *weak atrium/atrial myosin heavy chain* disrupts atrial function and influences ventricular morphogenesis in zebrafish. *Development* **130**, 6121-6129.

Hanks, S. K. and Hunter, T. (1995). Protein kinases 6. The eukaryotic protein kinase superfamily: kinase (catalytic) domain structure and classification. *FASEB J.* **9**, 576-596.

Horne-Badovinac, S., Lin, D., Waldron, S., Schwarz, M., Mbamalu, G., Pawson, T., Jan, Y., Stainier, D. Y. and Abdelilah-Seyfried, S. (2001). Positional cloning of *heart and soul* reveals multiple roles for PKC lambda in zebrafish organogenesis. *Curr. Biol.* **11**, 1492-1502.

Horne-Badovinac, S., Rebagliati, M. and Stainier, D. Y. (2003). A cellular framework for gut-looping morphogenesis in zebrafish. *Science* **302**, 662-665.

Huang, C. J., Tu, C. T., Hsiao, C. D., Hsieh, F. J. and Tsai, H. J. (2003). Germ-line transmission of a myocardium-specific GFP transgene reveals critical regulatory elements in the *cardiac myosin light chain 2* promoter of zebrafish. *Dev. Dyn.* **228**, 30-40.

Hurd, T. W., Gao, L., Roh, M. H., Macara, I. G. and Margolis, B. (2003). Direct interaction of two polarity complexes implicated in epithelial tight junction assembly. *Nat. Cell Biol.* **5**, 137-142.

Jowett, T. and Lettice, L. (1994). Whole-mount in situ hybridizations on zebrafish

embryos using a mixture of digoxigenin- and fluorescein-labelled probes. *Trends Genet.* **10**, 73-74.
Kimmel, C. B., Ballard, W. W., Kimmel, S. R., Ullmann, B. and Schilling, T. F. (1995). Stages of embryonic-development of the Zebrafish. *Dev. Dyn.* **203**, 253-310.
Nam, S. C. and Choi, K. W. (2003). Interaction of Par-6 and Crumbs complexes is essential for photoreceptor morphogenesis in *Drosophila*. *Development* **130**, 4363-4372.
Peterson, R. T., Mably, J. D., Chen, J. N. and Fishman, M. C. (2001). Convergence of distinct pathways to heart patterning revealed by the small molecule concentramide and the mutation *heart and soul*. *Curr. Biol.* **11**, 1481-1491.
Picker, A., Brennan, C., Reifers, F., Clarke, J. D. W., Holder, N. and Brand, M. (1999). Requirement for the zebrafish mid-hindbrain boundary in midbrain polarisation, mapping and confinement of the retinotectal projection. *Development* **126**, 2967-2978.
Shepard, J. L., Stern, H. M., Pfaff, K. L. and Amatruda, J. F. (2004). Analysis of the cell cycle in zebrafish embryos. *Methods Cell Biol.* **76**, 109-125.
Stainier, D. Y., Lee, R. K. and Fishman, M. C. (1993). Cardiovascular development in the zebrafish. I. Myocardial fate map and heart tube formation. *Development* **119**, 31-40.
Stainier, D. Y., Weinstein, B. M., Detrich, H. W., III, Zon, L. I. and Fishman, M. C. (1995). *cloche*, an early acting zebrafish gene, is required by both the endothelial and hematopoietic lineages. *Development* **121**, 3141-3150.
Thermes, V., Grabher, C., Ristoratore, F., Bourrat, F., Choulika, A., Wittbrodt, J. and Joly, J. S. (2002). I-SceI meganuclease mediates highly efficient transgenesis in fish. *Mechanisms of Development* **118**, 91-98.
Trinh, L. A. and Stainier, D. Y. (2004). Fibronectin regulates epithelial organization during myocardial migration in zebrafish. *Dev. Cell* **6**, 371-382.
Trinh, L. A., Yelon, D. and Stainier, D. Y. R. (2005). Hand2 regulates epithelial formation during myocardial differentiation. *Curr. Biol.* **15**, 441-446.
Wang, Q., Hurd, T. W. and Margolis, B. (2004). Tight junction protein Par6 interacts with an evolutionarily conserved region in the amino-terminus of PALS1/stardust. *J. Biol. Chem.* **279**, 30715-30721.
Wei, X. and Malicki, J. (2002). *nagie oko*, encoding a MAGUK-family protein, is essential for cellular patterning of the retina. *Nat. Genet.* **31**, 150-157.
Westerfield, M. (1994). *The Zebrafish Book* (ed. M. Westerfield). Oregon: University of Oregon Press.
Yelon, D., Horne, S. A. and Stainier, D. Y. (1999). Restricted expression of cardiac myosin genes reveals regulated aspects of heart tube assembly in zebrafish. *Dev. Biol.* **214**, 23-37.